AIAA-2005-4400

Laser-Induced Fluorescence of Neutral Xenon in the Near Field of a 200 W Hall Thruster

William A. Hargus, Jr.*
Air Force Research Laboratory
Spacecraft Propulsion Branch
Edwards AFB, CA 93524

Abstract

This work presents measurements of neutral xenon velocity in the plume of the Busek Company BHT-200-X3 200 W Hall thruster at a single 250 V anode potential operating condition. The xenon velocities were measured using laser induced fluorescence of the $6s'[1/2]_1^0 - 6p'[3/2]_2$ excited state transition at 834.68 nm. Velocities were interrogated near the exit plane of the anode discharge and in the vicinity of the cathode. Both axial and radial velocities were measured simultaneously using phase sensitive detection. The exit plane axial velocity varies from 350–50 m/s near the outer acceleration channel radius to approximately 150 m/s at the inner radius. The radial velocity at the outer insulator is approximately zero, but increases to approximately 100 m/s directed away from the protruding central magnetic pole at the inner insulator. This is consistent with the creation of neutrals at the inner radius by ions neutralized following a wall collision with the protruding central magnetic pole. Neutral velocities downstream of the exit plane also show a radial velocity away from the central magnetic pole. However, this behavior may be due to the influence of the cathode plume. Velocity measurements in the cathode plume show that xenon velocities reach in excess of 610 m/s. Since the cathode flow represents a substantial portion of the thruster flow and is only weakly ionized, the cathode plume may influence the neutral velocities nearer the anode. Evidence of interaction between the two flows takes the form of widened fluorescence line profiles which may indicate the collisional mixing disparate neutral streams or possibly several gas dynamic shocks.

Introduction

The goal of this study is to measure the neutral xenon (Xe I) velocity field of a 200 W Hall thruster using excited state atomic xenon laser induced fluorescence (LIF). Unlike ions, atoms can not be characterized by electrostatic probes. Often, LIF is the preferred diagnostic for the investigation of various plasma species since it is a non-intrusive measurement. Unlike electrostatic probes, LIF will not perturb the local plasma, or thruster operation. In this particular case, LIF appears to be the only practical measurement method.

Hall thrusters produce thrust by the acceleration of ions through an electric field. Xenon is used as a propellant due to its high atomic mass, inert chemistry, and low ionization energy. Xenon ions will exit Hall thrusters at ~15 km/s. A fraction of the xenon propellant is not ionized, and is not accelerated. A well known loss mechanism, these neutrals probably represent less than 10% of the propellant flow. However, their density is comparable to ionic flow due to the wide difference in velocities.

Understanding the behavior of the neutral flow is important for the complete characterization of Hall thrusters. For example, high neutral densities influence electron transport by providing collision partners for low energy electrons seeking to cross magnetic field lines. Neutrals are also a source of charge exchange collision partners with the ion stream. Charge exchange may be responsible for the creation of highly divergent low energy ions which influence Hall thruster spacecraft integration. In addition, how the neutrals flowing though the thruster interact with the background neutrals in ground test facilities is a growing concern. Understanding the differences between ground test and on-orbit thruster operation is an emerging area of study.

Complicating neutral flow measurements from the anode discharge plume is a high density jet of neutrals from the hollow cathode neutralizer which represents approximately 10% of the total thruster propellant flow. Unlike the anode flow, the hollow cathode plume is only weakly ionized. The cathode produces a high density jet of neutrals which may also influence the flow

*Research Engineer AFRL, Senior member AIAA

Report Documentation Page

Public reporting burden for the collection of information is estimated to average 1 hour per response, including the time for reviewing instructions, searching existing data sources, gathering and maintaining the data needed, and completing and reviewing the collection of information. Send comments regarding this burden estimate or any other aspect of this collection of information, including suggestions for reducing this burden, to Washington Headquarters Services, Directorate for Information Operations and Reports, 1215 Jefferson Davis Highway, Suite 1204, Arlington VA 22202-4302. Respondents should be aware that notwithstanding any other provision of law, no person shall be subject to a penalty for failing to comply with a collection of information if it does not display a currently valid OMB control number.

1. REPORT DATE **JUN 2005**	2. REPORT TYPE	3. DATES COVERED **-**

4. TITLE AND SUBTITLE **Laser-Induced Fluorescence of Neutral Xenon in the Near Field of a 200 W Hall Thruster**	5a. CONTRACT NUMBER
	5b. GRANT NUMBER
	5c. PROGRAM ELEMENT NUMBER
6. AUTHOR(S) **William Hargus, Jr.**	5d. PROJECT NUMBER **2308**
	5e. TASK NUMBER **0535**
	5f. WORK UNIT NUMBER

7. PERFORMING ORGANIZATION NAME(S) AND ADDRESS(ES) **Air Force Research Laboratory (AFMC),AFRL/PRSS,1 Ara Road,Edwards AFB,CA,93524-7013**	8. PERFORMING ORGANIZATION REPORT NUMBER

9. SPONSORING/MONITORING AGENCY NAME(S) AND ADDRESS(ES)	10. SPONSOR/MONITOR'S ACRONYM(S)
	11. SPONSOR/MONITOR'S REPORT NUMBER(S)

12. DISTRIBUTION/AVAILABILITY STATEMENT
Approved for public release; distribution unlimited

13. SUPPLEMENTARY NOTES

14. ABSTRACT
This work presents measurements of neutral xenon velocity in the plume of the Busek Company BHT-200-X3 200 W Hall thruster at a single 250 V anode potential operating condition. The xenon velocities were measured using laser induced fluorescence of the 6s'[1/2]0/1 -6p'[3/2]2 excited state transition at 834.68 nm. Velocities were interrogated near the exit plane of the anode discharge and in the vicinity of the cathode. Both axial and radial velocities were measured simultaneously using phase sensitive detection. The exit plane axial velocity varies from 350-50 m/s near the outer acceleration channel radius to approximately 150 m/s at the inner radius. The radial velocity at the outer insulator is approximately zero, but increases to approximately 100 m/s directed away from the protruding central magnetic pole at the inner insulator. This is consistent with the creation of neutrals at the inner radius by ions neutralized following a wall collision with the protruding central magnetic pole. Neutral velocities downstream of the exit plane also show a radial velocity away from the central magnetic pole. However, this behavior may be due to the influence of the cathode plume. Velocity measurements in the cathode plume show that xenon velocities reach in excess of 610 m/s. Since the cathode flow represents a substantial portion of the thruster flow and is only weakly ionized the cathode plume may influence the neutral velocities nearer the anode. Evidence of interaction between the two flows takes the form of widened fluorescence line profiles which may indicate the collisional mixing disparate neutral streams or possibly several gas dynamic shocks.

15. SUBJECT TERMS

16. SECURITY CLASSIFICATION OF:			17. LIMITATION OF ABSTRACT	18. NUMBER OF PAGES	19a. NAME OF RESPONSIBLE PERSON
a. REPORT **unclassified**	b. ABSTRACT **unclassified**	c. THIS PAGE **unclassified**		**9**	

field in the vicinity of the anode. This flow of neutrals may affect local electron conductivity and hence plume neutralization. As a result, the cathode plume may also influence insulator erosion patterns, particularly in the case of very high power Hall thrusters.

Xenon Spectroscopy

The nine stable isotopes of xenon each have a slight difference in their electron transition energies due to their differences in mass. The odd mass isotopes are further spin split due to nuclear magnetic dipole and electric quadrapole moments. Nuclei which have an odd number of protons and/or an odd number of neutrons possess an intrinsic nuclear spin $Ih/2\pi$, where I is integral or half-integral depending on whether the atomic mass is even or odd, respectively. For nuclei with non-zero nuclear spin (angular momentum), there exists an interaction of the nucleus with the electron shell. This interaction leads to the splitting of levels with angular momentum J into a number of components, each corresponding to a specific value of the total angular momentum F. The details of how hyperfine spin splitting affects the spectra of xenon are described in more detail elsewhere [1].

For the results reported here, the $6s'[1/2]_1^0 - 6p'[3/2]_2$ electronic transition of Xe I at 834.68 nm is probed. The isotopic and nuclear-spin effects contributing to the hyperfine structure of the $6s'[1/2]_1^0 - 6p'[3/2]_2$ xenon ion transition produce a total of 18 isotopic and spin split components. The hyperfine splitting constants which characterize the variations in state energies are only known for a limited number of energy levels.

It is not presently known whether hyperfine and isotopic constants have been measured for the $6s'[1/2]_1^0 - 6p'[3/2]_2$ transition. Therefore, it is not presently possible to model the lineshape to determine temperature and/or pressure broadening parameters. For velocity measurements, it is convenient to probe optically accessible transitions. The incomplete knowledge of the isotopic and nuclear spin splitting constants does not affect the determination of velocity. A convenient feature of this line is its proximity to the $5d[3]_{7/2} - 6p[2]_{5/2}$ ionic transition (~17 GHz separation). This fact allows for the same optics and laser to be used to probe either transition with only small procedural adjustments.

Another fortunate feature of the $6s'[1/2]_1^0 - 6p'[3/2]_2$ transition is the presence of a relatively strong line originating from the same upper state ($6s[3/2]_1^0 - 6p'[3/2]_2$ transition at 473.42 nm [2,3]) which allows for nonresonant fluorescence collection. A nonresonant fluorescence scheme is preferred where there is the possibility of laser scattering from surfaces.

The velocity of the sample volume is determined by measurement of the Doppler shift of the absorbing atoms. If an absorber has a velocity component u along the axis of the laser beam, it will absorb the light at a frequency shifted from that of stationary absorbers. The magnitude of this frequency shift δv_{12} depends on the speed u along the laser beam axis

$$\delta v_{12} = v_{12}\frac{u}{c}$$

where c is the speed of light. The Doppler shift of a species fluorescence profile away from the line center v_{12} of stationary absorbers is in proportion to u [4].

Apparatus

The measurements in this effort were performed in Chamber 6 of the Air Force Research Laboratory (AFRL) Electric Propulsion Laboratory at Edwards AFB, CA. Chamber 6 is a nonmagnetic stainless steel chamber which has a 1.8 m diameter and 3 m length. It has a measured pumping speed of 32,000 l/s on xenon. Pumping is provided by four single stage cryo-panels (single stage cold heads at ~25 K) and one 50 cm two stage cryo-pump (<12 K). Chamber pressure during thruster operation is approximately 5×10^{-6} Torr, corrected for xenon.

Table 1: Nominal Thruster Operating Conditions

Anode flow	840 μg/s (Xe)
Cathode flow	98 μg/s (Xe)
Anode potential	250 V
Anode current	0.820 A
Keeper current	0.5 A
Magnet current	0.75 A
Heater current	3.0 A

The Hall thruster is the Busek Company BHT-200-X3 200 W Hall thruster which has been described elsewhere [5]. Table 1 shows the nominal operating conditions for the BHT-200-X3 thruster for this test. During thruster operation, the parameters shown in Table 1 are monitored and recorded at a 1 Hz data rate. It should be
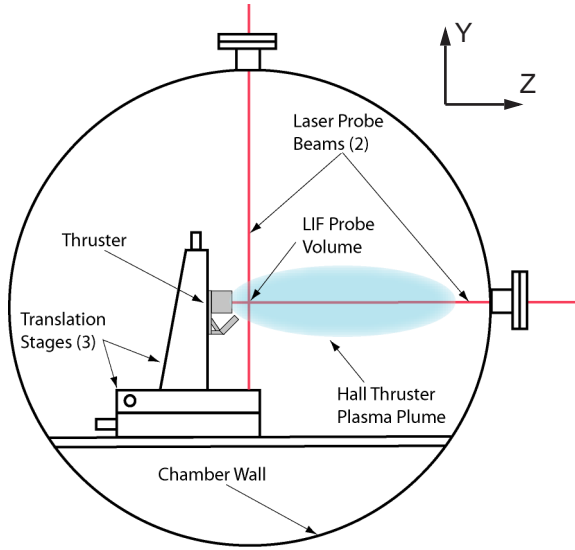
Fig. 1. Side view diagram of thruster within AFRL chamber 6. Also shown are the translation stages and the laser probe beams. Note that the fluorescence collection and external optics are not shown.

noted that compared to previous ion velocity measurements [6], the magnetic field strength was reduced due to plasma oscillations which affected stable thruster operation. These appear to be a function of thruster ageing and are eliminated by a slight reduction of the magnetic field.

Figure 1 shows a side-view diagram of the Hall thruster mounted within the vacuum chamber. The thruster is mounted on a three axes orthogonal computer controlled translation system. Figure 1 also shows the two orthogonal LIF probe beams and windows through which the beams enter the chamber. Figure 2 shows a top view of the laser optical train, collection optics, and one leg of the external probe optics.

The laser used is a New Focus Vortex tunable diode laser. It is capable of tuning approximately –50 GHz about a center wavelength of 834.7 nm. The 10 mW beam is passed through a Faraday isolator to eliminate feedback to the laser. The laser beam then passes through several beam pick-offs until it reaches a 50-50 beam splitter (BS) where it is split into two beams of equal power. The first beam, the axial probe beam shown in Figs. 1 and 2, is focused by a lens and enters the vacuum chamber through a window. A second probe beam, shown in Fig. 1 only, is directed from the optical bench via a periscope apparatus so that it enters the chamber from above the thruster and probes the velocity
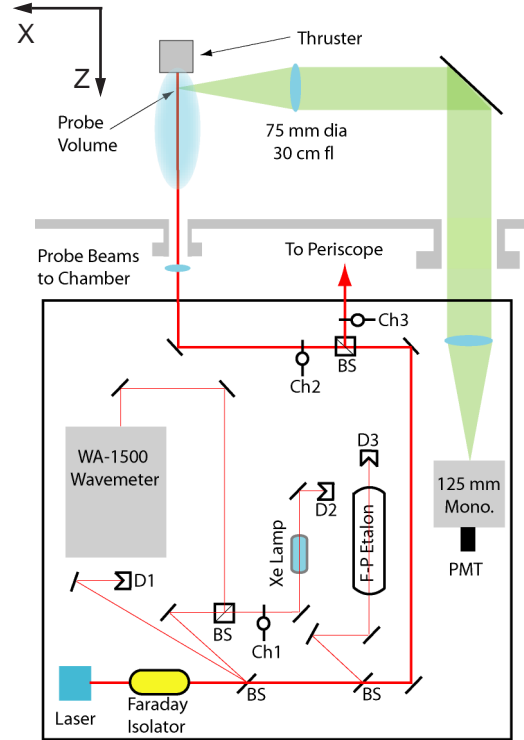

Fig. 2. Top view diagram of the laser optical train and collection optics. Note that the radial probe beam periscope and focusing optics are not shown.

perpendicular to the first probe beam. Each probe beam is chopped at a unique frequency by choppers Ch2 (2.8 kHz) and Ch3 (2.0 kHz) for simultaneous phase sensitive detection of the two fluorescence signals.

The two wedge beam pick-offs (/BS) shown in Fig. 2 provide portions of the beam for diagnostic purposes. The first beam pick-off directs a beam to a photodiode detector (D1) used to provide constant power feedback to the laser. The second beam is divided into two equal components by a 50-50 cube beam splitter. The first component is directed to an Burleigh WA-1500 wavemeter used to monitor absolute wavelength. The second component is sent through a chopper Ch1 (1.3 kHz) and through a low pressure xenon hollow cathode discharge lamp. The lamp provides a stationary absorption reference for the direct determination of the Doppler shift $\delta\nu_{12}$. The second pick-off sends a beam to a 300 MHz free spectral range Fabry-Perot etalon (F-P). This instrument provides high resolution frequency monitoring of the wavelength interval swept during a laser scan.

The fluorescence collection optics are also shown in Fig. 2. The fluorescence is collected by a 75 mm diameter, 300 mm focal length lens within the chamber. The collimated fluorescence signal is directed through a window in the chamber side wall to a similar lens that focuses the collected fluorescence onto the entrance slit of 125 mm focal length monochrometer with a Hamamatsu R928 photomultiplier tube (PMT) detector. Due to the 1:1 magnification of the collection optics, the spatial resolution of the measurements is determined by the geometry of the entrance slit 1 mm width and 1.7 mm height as well as the sub-mm diameter of the probe beams.

The laser is controlled by an analog ramp signal generated by a National Instruments E-series data acquisition board. During each laser scan, the data acquisition card records the absorption and two fluorescence signals using three lockin amplifiers. The signal from the Fabry Perot etalon photodiode detector (D3) signal is amplified and filtered using a current pre-amplifier. The output of which is also recorded. Typically, the scans span 6 GHz. Each scan yields four traces of several thousand points. The traces are then stored for analysis.

The data analysis procedure consists of first normalizing the wavelength interval using the Fabry-Perot etalon trace. Subsequently, the reference absorption trace is rectified by subtraction of the absorption baseline. The Doppler shifts of the LIF signal relative to the absorption signal are then calculated by two methods. The first fits an estimated lineshape to each curve and determines the Doppler shift from the calculated line centers. The second method is a numerical cross-correlation which compares the absorption and LIF line shapes to determine the Doppler shift. It is much less sensitive to signal noise and is more mathematically rigorous than the first method. However, both methods typically produced very similar results. Measurement uncertainties are determined from the differences between the two methods as well as from statistics of repeated measurements. Typically uncertainties are greatest near the main discharge due to low signal strength and least near the cathode where the signal is much higher. As a result, the LIF scans nearest the anode typically integrated for 20-25 min., while the scans taken nearest the cathode integrated for less than 5 minutes. In addition, radial measurements near the anode discharge exit sometimes exhibit a particularly wide LIF line profile which cause these measurements to have the greatest variability. For the measurements presented here, the uncertainty is estimated to be
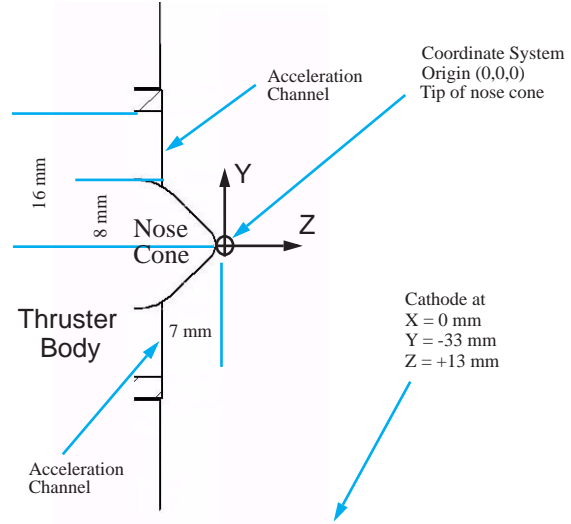

Fig. 3. Near field dimensions of the BHT-200 with origin of the coordinate system and positions of important locations noted.

approximately –50 m/s, but is probably lower for the axial measurements.

Figure 3 shows the near field geometry of the Busek BHT-200 Hall thruster. The locations of the protruding central magnetic pole (nose cone) and edges of the acceleration channel are indicated as is the position of the cathode exit. The cartesian coordinate system and origin used in these measurements are also shown in Fig. 3. The coordinate system orientation is also referenced in Figs. 1 and 2. The origin is at the tip of the nose cone due to the ease and repeatability with which this position is located. All measurements are identified using these coordinates. Measurements presented in this work will be limited to the Y-Z plane. Therefore in the anode discharge exit region, the Y axis velocity measurements correspond to the radial velocities, and the Z axis measurements to the axial.

Experimental Results

Figure 4 shows sample LIF and rectified absorption traces used to determine the velocity components of accelerated xenon neutrals taken at the cathode exit at Y = -33 mm and Z = +13 mm. The right-most lineshape is the rectified absorption trace (0 m/s), the center lineshape is the axial signal (135 m/s), and the left-most lineshape is the radial signal (340 m/s). The signal at the cathode exit is highest signal strength encountered. Similar signals in the vicinity of the anode discharge exit plane required 10x longer time constants to achieve comparable signal to noise ratios (SNR) and
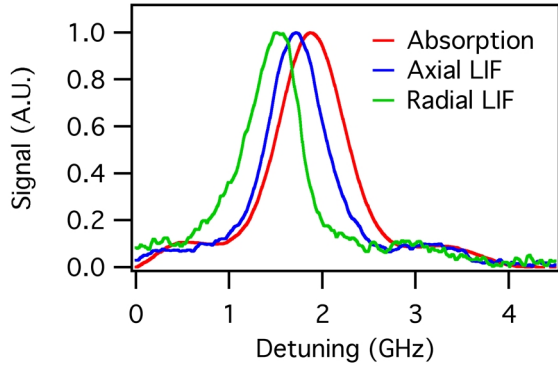
Fig. 4. Typical LIF and rectified absorption trace used to determine velocity. This particular data trace is from the cathode exit (Y = -33 mm, 340 m/s; Z = 13 mm, 135 m/s).

several cases required 30x. This limited data from the anode plume.

Anode Exit Plane Region

Figure 5 shows the axial and radial velocities at the anode discharge exit plane. The upper toroidal portion (see Fig. 3) is the only portion of the anode plume where velocity measurements are available to the geometry of the protruding central magnetic pole. The Xe I velocity is nearly completely axial along the outer radius of the discharge channel (Y = 16 mm). The axial velocity component diminishes toward the central magnetic pole and the radial velocity component appears to increase.

This trend is mirrored by the Gaussian fit profile width of the LIF profile shown in Fig. 6. The profile width of both velocity components increases consistently with proximity to the protruding boron nitride capped central magnetic pole. Despite lack of knowl-
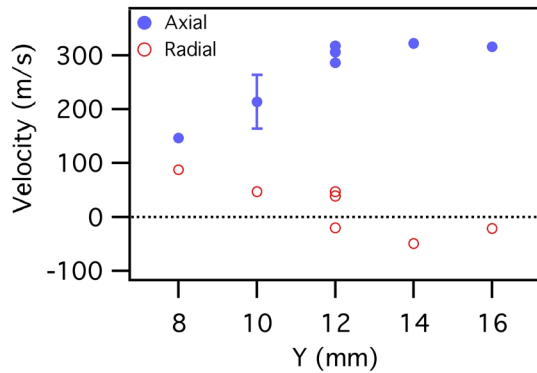
edge of the lineshape function, the square of the linewidth is related to the temperature (e.g. random thermal energy) [4]. It therefore appears that the temperature of the neutrals is significantly higher; perhaps as much as 5x across the width of the acceleration channel.

Simply using the radial LIF profile width to calculate a maximum temperature (simplistically assuming purely Doppler broadening, neglecting all other broadening mechanisms), the temperature ranges from 7,500 K at the central pole to 1,500 K at the outer radius. As a reference, the lamp discharge profile produces an apparent temperature of 1,300 K. These estimates ignore the complex spectra of xenon as well as any pressure broadening mechanisms and represent an absolute maximum temperature.

It appears likely that neutrals are being created by ion collision/neutralization on the boron nitride surface of the protruding central magnetic pole. These neutrals can not be differentiated from the never ionized neutrals. The combination of these two populations could produce broadened velocity distributions similar to those seen here. Alternatively, plasma densities may be higher near the central pole and could be responsible at least some of the broadening.

Figure 7 shows Xe I velocities at the center of the acceleration channel (Y = 12 mm) extending from the exit plane (Z = -7 mm) to 5 mm beyond the tip of the central magnetic pole (Z = +5 mm). Both the axial and radial velocity components are invariant to the precision of the measurement. Figure 8 shows the LIF profile widths of the axial and radial LIF signals with the profile width of the absorption trace as a reference. The radial profile width decreases as would be expected

Fig. 5. Exit plane velocity components at the exit plane. Note error bar denoting calculated uncertainty in the velocity measurements.
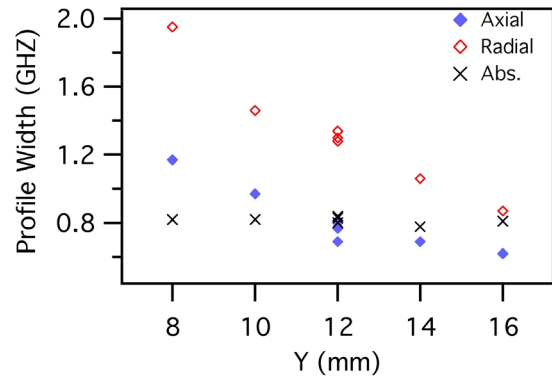

Fig. 6. Exit plane LIF profile widths (GHz) for both axial and radial traces. As a reference, the profile width of the absorption trace is also shown.
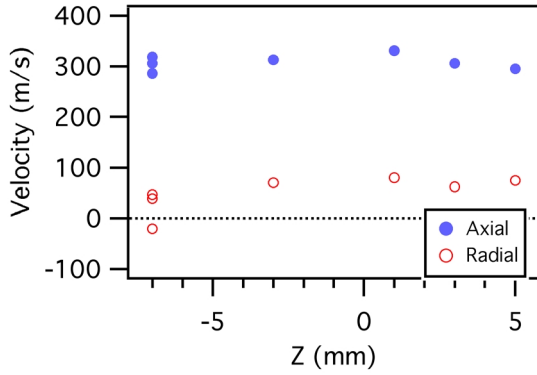
5

Fig. 7. Velocity components along the accelera-tion channel centerline (Y = 12 mm) extending from the exit plane (Z = -7 mm) to Z = 5 mm.

from an expanding, cooling flow. Initially, the axial pro-file also narrows, although only slightly. Beyond the tip of the central magnetic pole, the profile increases sud-denly. It does not appear to be an artifact of the data, and SNR of the signal is not significantly different in this region. A possible explanation is interaction from the neutral flow from beneath the central pole, either from the opposite portion of the toroidal channel, or from the cathode plume. Alternatively, the effect may be the result of a gas dynamic shock produced by the interac-tion of an over-expanded anode plume interacting with the background neutrals.

Figure 9 contains axial and radial velocities at the outer insulator radius (Y = 16 mm) extending from the exit plane (Z = -7 mm) to 3 mm beyond the central magnetic pole tip (Z = 3 mm). The data is very similar to that of the acceleration channel center line data shown in Fig. 7. The axial velocity is nearly constant at approx-
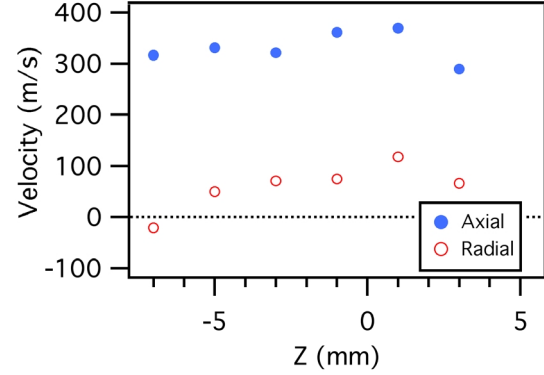

Fig. 8. LIF profile widths (GHz) for both axial and radial traces along the centerline of the acceleration channel (Y = 12 mm). As a refer-ence, the profile width of the absorption trace is also shown.

Fig. 9. Velocity components along the acceler-ation channel outer radius (Y = 16 mm) extending from the exit plane (Z = -7 mm) to Z = 3 mm.
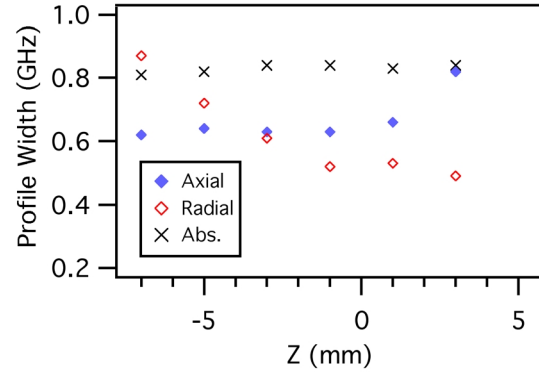

Fig. 10. LIF profile widths (GHz) for both axial and radial traces along the outer radius of the acceleration channel (Y = 16 mm). As a reference, the profile width of the absorption trace is also shown.
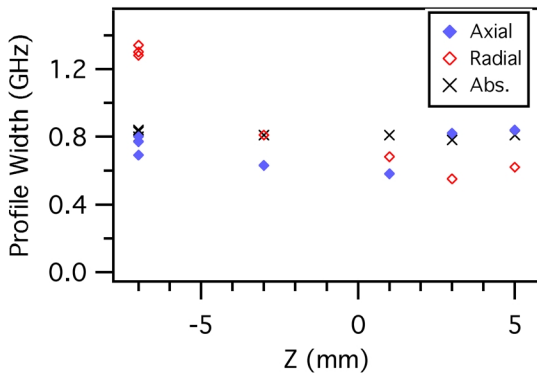
imately 300 m/s. The radial velocity exhibits more vari-ation than the previous case, but the behavior is similar with an average velocity of approximately 75 m/s. The corresponding LIF profile widths are shown in Fig. 10. Similar to the acceleration channel center velocities shown in Fig. 8, the LIF profile width of the radial sig-nal drops with distance from the exit plane, typical of an expanding, cooling flow. In congruence with the previ-ous data, the axial profile width is near constant until Z = 3 mm, beyond which it rises by nearly 25%.

Cathode Region

The hollow cathode consumes approximately 10% of the total thruster propellant flow. The cathode flow supports the cathode discharge and cools the cath-ode to prevent evaporation of the low work function electron emitting materials. Due to the restrictive geom-etry and low ionization fraction, the neutral xenon den-

sity is significantly higher at the cathode than at the main discharge exit, by an estimated 20x.

Figure 11 is a vector plot of the velocity flow field in the cathode as well as the near exit plane regions. At the cathode exit, the neutral velocity is 380 m/s. The remainder of the flow appears to be a gas dynamic expansion. The peak velocity measured in the upper right hand portion of the cathode flow region is approximately 610 m/s. Interestingly, the maximum is not centered on the initial jet. This is more apparent in Fig. 12 where the cathode region velocity field is shown in greater detail. The individual points where velocity data is available are denoted by the arrow origins. The contours show the interpolated velocity magnitude. Interestingly, the velocity field does not develop symmetrically about the cathode exit. The velocity field is skewed away from the anode discharge. The cathode plume appears to be interacting with the anode plume.

Some evidence of the interaction of the anode and cathode plumes is shown in Figs. 13 and 14. These show the Z and Y lineshape profile widths. (Note in previous discussion, these were denoted as axial and radial, respectively. This terminology in the cathode plume is not appropriate due to the geometry.) Figure 13 contours show the Z axis LIF profile width as it varies with the cathode plume expansion. It shows an expansion where the profile width is lessening as the flow expands and cools. There appears to be a sudden rise downstream of the cathode; however, this feature is due to a single data point and may be questionable.

Figure 14 shows the Y axis LIF profile width in the near cathode region. From the interpolated profile contours, it appears that the cathode plume contains several features, possibly shocks, which turn the flow to the right. Taken together, Figs. 13 and 14 imply that the cathode plume is interacting with either the anode plume or the background neutrals in the vacuum chamber (background pressure ~5x10^{-6} Torr). This interaction appears as a select broadening of the LIF profiles. It may indicate that there is mixing of varied velocity distributions, or that a gas dynamic shock is present. Due to the sparseness of the available data, there is considerable uncertainty as to what is producing the increased LIF profile width, but it indicates that the anode and cathode neutral plumes exhibit unexpected complexity.

Conclusions

This effort demonstrates neutral xenon velocity measurements in the exit plane and cathode regions of a 200 W low power Hall thruster. The
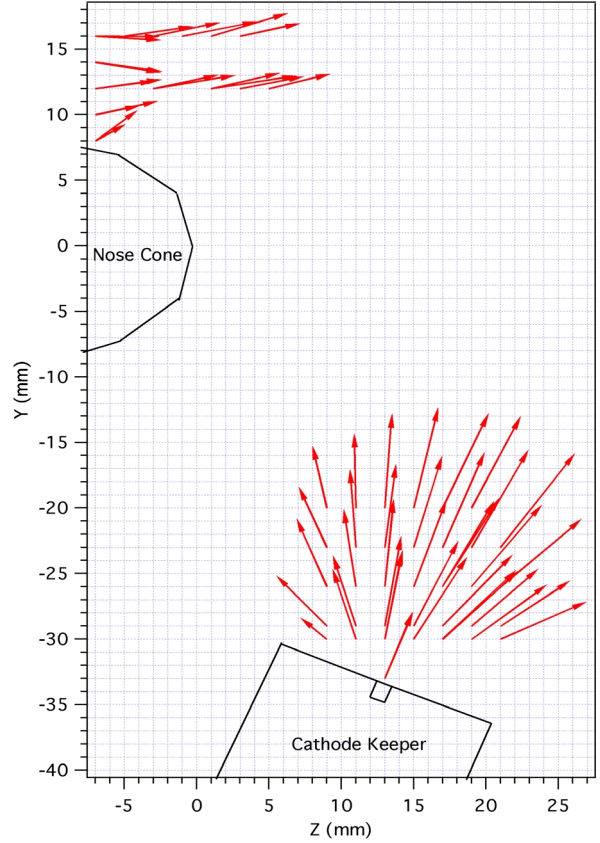

Fig. 11. Neutral xenon vector flow field in the thruster exit and cathode regions.
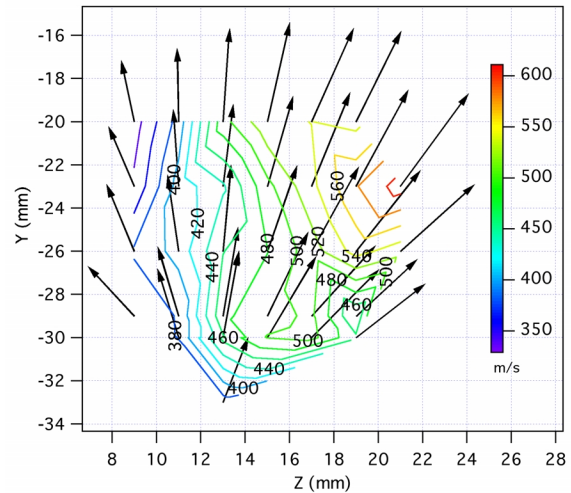

Fig. 12. Neutral xenon flow field in the cathode region. Contours denote velocity magnitude.

$6s'[1/2]_1^0 - 6p'[3/2]_2$ xenon transition used in this study is optically accessible using relatively inexpensive diode lasers and is approximately 17 GHz from the $5d[3]_{7/2} - 6p[2]_{5/2}$ ionic transition previously used to measure xenon ion velocities [1,6]. Although not all transition spectral constants are known for either transi-
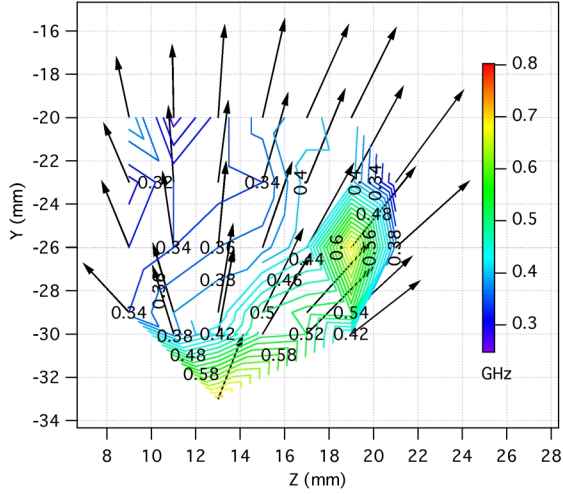
Fig. 13. Cathode plume Z axis LIF profile width contours with velocity vectors overlayed. Note the general cooling trend.
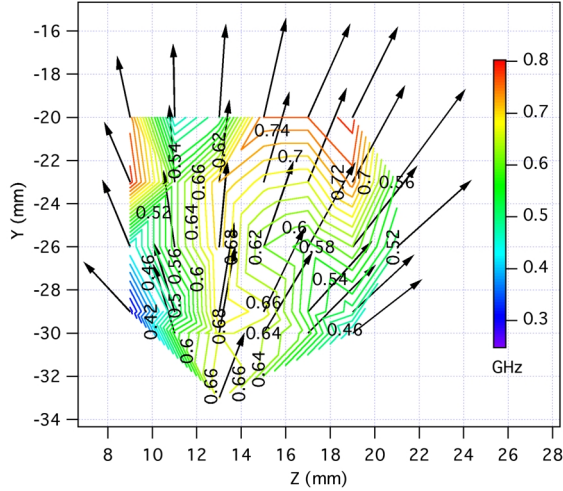

Fig. 14. Cathode region Y axis LIF profile width contours with velocity vectors overlayed. Note the apparent interaction with the anode plume

tion, their proximity allows for the same experimental apparatus to be used to acquire both neutral and ionic velocity data with minimal adjustments.

At the main discharge exit plane, there is a pronounced neutral velocity away from the protruding central magnetic pole. The axial velocity is nearly invariant (~300 m/s) downstream until just beyond the central magnetic pole where a sudden increase in the LIF profile width occurs. It is not precisely understood what occurs at this location, but it is possible that it is caused by mixing with the cathode plume, or with the background neutrals. It is also possible that this feature is the
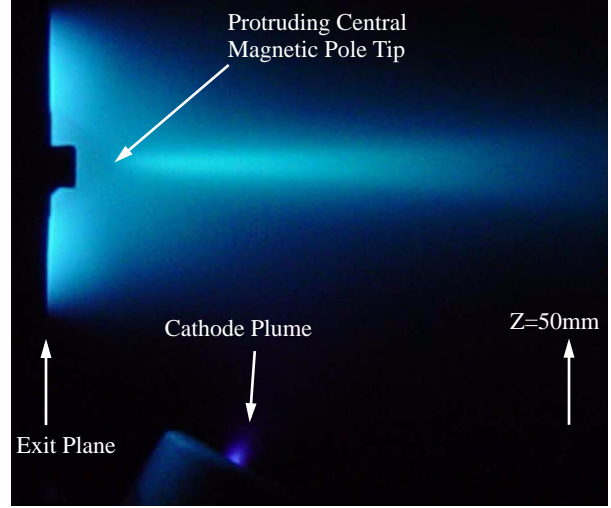

Fig. 15. Photograph of the BHT-200 Hall thruster plume operating at nominal conditions with various features identified.

result of a shock; however, there is insufficient data to confirm any of these possibilities.

Due to the low degree of ionization, the cathode plume has the highest concentration of xenon neutrals. The cathode plume exhibits considerable acceleration. The velocity measured at the cathode exit is approximately 380 m/s and the peak velocity measured further downstream is 610 m/s. The cathode plume appears to be slightly skewed by interaction with the anode plume. Using the LIF profile widths as a metric, there may be several oblique shocks where the cathode and anode plumes interact. However, the sparse data indicates that caution should be taken in this analysis.

Figure 15 is a photograph of the BHT-200-X3 Hall thruster at AFRL. Previous ion velocity surveys have determined that the visibly luminous portions of the plasma correspond to locations with mixing of separate ion velocity populations [6]. The luminous areas nearest the main discharge and visible cathode jet qualitatively appear to correlate with the LIF profile width features which are postulated to be gas dynamic shocks. It is apparent that more measurements and analysis are required before these artifacts are fully understood.

Cappelli et al. performed a series of ground state neutral density measurements using self absorption in the vacuum ultra violet [7]. These measurements support the supposition that there is considerable interaction between the anode and cathode plumes. The density measurements also show an anomalous rise in neutral plume density directly downstream of the anode cen-

8

tered near the cathode plane. This feature is identified by the density measurements as a possible gas dynamic shock. This hypothesis appears to support the conclusions drawn from LIF profile widths in this work. It appears obvious that the neutral flow in the near field of a Hall thruster is a complex interaction of a diffuse plume form the main discharge and a more concentrated jet from the cathode. The degree to which this system interacts with the ion flow from the main discharge remains an open question.

Future efforts will concentrate on understanding how to interpret the differences in LIF profile width in the plume. It is not obvious how these are to be interpretated. It would also be interesting to compare these results to numerical model results. Such an integrated study of the near anode and near cathode regions could provide valuable insights into the physics of the flow interactions. It may also be necessary to repeat these measurements for a transition where all the spectral constants are known, including the hyperfine structure. Cedolin pioneered the use of the $6s[3/2]_2^0 - 6p[3/2]_2$ transition at 823.2 nm for this use and developed a sophisticated line shape model [8].

Acknowledgements

References

1. W. A. Hargus, Jr. and M. A. Cappelli, Laser-Induced Fluorescence Measurements of Velocity within a Hall Discharge, *Applied Physics B,* Vol. 72, pp 961-969, 2001.

2. M.H. Miller and R.A. Roig, Transition Probabilities of Xe I and Xe II, *Physical Review A,* Vol. 8, pp 480-486, July 1973.

3. C.E. Moore, *Atomic Energy Levels: Volume II,* Washington: National Bureau of Standards, pp 113-123, 1958.

4. W. Demtroder, *Laser Spectroscopy: Basic Concepts and Instrumentation,* Springer-Verlag, Berlin, 1996

5. W.A. Hargus, Jr. and G. Reed, The Air Force Clustered Hall Thruster Program, AIAA-2002-3678, *38th Joint Propulsion Conference,* 7-10 July 2002, Indianapolis, Indiana.

6. W.A. Hargus, Jr. and C.S. Charles, Near Exit Plane Velocity Field of a 200 W Hall Thruster, AIAA-2003-5154, *39th Joint Propulsion Conference,* 20-23 July 2003, Huntsville, AL.

7. M. A. Cappelli and W. A. Hargus, Jr., Images of Ground State Xenon Density in the Near Field of Low Power Hall Thruster, AIAA-2004-4120, *40th Joint Propulsion Conference,* 11-14 July 2004, Fort Lauderdale, FL.

8. R.J. Cedolin, *Laser-Induced Fluorescence Diagnostics for Xenon Plasmas,* Ph.D. Dissertation, Mechanical Engineering, Stanford University, June 1997.